VISCOUS FLOW IN SLOTS

Wolfgang Geller
Deutsche Forschungs- und Versuchsanstalt
fuer Luft- und Raumfahrt E.V.
Cologne, West Germany

Abstract

The incompressible laminar flow past a flat plate moving at a small distance parallel to the ground is investigated theoretically. The flow field is calculated by numerical integration of the vorticity transport equation and the Poisson equation for the streamfunction. Computed pressure and shear stress distribution along the ground and on the plate surface are given for low Reynolds numbers and several distances between the lower surface of the plate and the ground.

Introduction

Dealing with the aerodynamics of high speed ground transportation vehicles one encounters flow regions between the moving body, and for instance, the fixed rail, or between a vertical standing track and an u-formed sledge. Theoretical work is done in order to investigate such flows and to develop prediction methods for the drag, and means of controlling the slot flow.

Problem

In order to study the flow in the region between the lower surface of the vehicle and the ground a simplified model is considered: A thin flat plate of length ℓ and thickness d moves parallel to the ground at a small distance h with a constant speed u_∞. The flow is assumed to be viscous, incompressible and twodimensional. In a coordinate system (x,y) being fixed on the plate the flow becomes stationary. Far upstream of the plate we have a parallel flow with constant velocity u_∞. The ground moves with the same speed underneath the plate

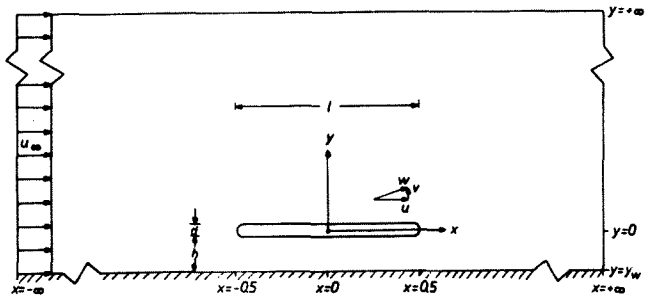

Fig.1 Flat plate in twodimensional incompressible viscous flow with ground effect.

(see Fig.1). Of most interest are the magnitude of the friction drag on the lower plate surface and the question, wether a pressure gradient is produced in the slot by the viscous effects of the flow.

Governing Equations

For the calculation of the flow field the vorticity transport equation for unsteady planar flows and the Poisson equation for the streamfunction are used:

$$\frac{\partial \omega}{\partial t} + \vec{w} \cdot \nabla \omega = \frac{1}{Re} \Delta \omega \qquad (1)$$

$$\Delta \psi = - \omega(x,y) \qquad (2)$$

All quantities in eqs.(1) and (2) are nondimensional. Denoting dimensional quantities by primes except for the reference values u_∞, ℓ, h, ν, ρ, p_∞, we have

time coordinate: $t = \frac{u_\infty t'}{\ell}$, abscissa: $x = \frac{x'}{\ell}$,

ordinate: $y = \frac{y'}{\ell}$, velocity: $\vec{w} = \frac{\vec{w}'}{u_\infty}$,

with components parallel to the x-axis:

$u = \frac{u'}{u_\infty} = \frac{\partial \psi}{\partial y}$ and parallel to the y-axis:

$v = \frac{v'}{u_\infty} = -\frac{\partial \psi}{\partial x}$, vorticity: $\omega = \frac{\partial v}{\partial x} - \frac{\partial u}{\partial y} = \frac{\ell \cdot \omega'}{u_\infty}$,

streamfunction $\psi = \frac{\psi'}{u_\infty \cdot \ell}$, Reynolds number,

with ν = kinematic viscosity: $Re = \frac{u_\infty \cdot \ell}{\nu}$.

An additional Reynolds number may be defined with the slot-heigth h:

$$Re_h = \frac{u_\infty \cdot h}{\nu} .$$

The variables ω and ψ of the stationary flow are found as asymptotic solutions for the transient flow for $t \to \infty$. Calculating the nondimensional pressure distribution

$$p = \frac{p' - p_\infty}{\rho u_\infty^2} \qquad (3)$$

(p_∞ being the dimensional local static pressure of the undisturbed flow far upstream of the plate, ρ the fluid density) a new variable, i.e. the nondimensional total pressure

$$p_T = \frac{p_T' - p_{T\infty}}{\rho u_\infty^2} = p + \frac{1}{2}(w^2 - 1) \qquad (4)$$

is introduced. The total pressure is expected to have a smoother distribution than the static pressure, thus being more suited for numerical treatment. Substituting eq.(4) into the Navier-Stokes-equation for the stationary flow

$$\nabla \frac{w^2}{2} - \vec{w} \times (\nabla \times \vec{w}) = -\nabla p - \frac{1}{Re} \nabla \times (\nabla \times \vec{w}) \qquad (5)$$

one gets

$$-\vec{w} \times (\nabla \times \vec{w}) = -\nabla p_T - \frac{1}{Re} \nabla \times (\nabla \times \vec{w}) , \qquad (6)$$

and after taking the divergence of eq.(6) we have a Poisson equation

$$\Delta p_T = \omega^2 - \nabla\psi \cdot \nabla\omega \qquad (7)$$

for the total pressure. The right hand side of eq.(7) are the solutions of eqs.(1) and (2) for the steady state case. Solving eq.(7) one obtains the total pressure, and the static pressure by application of eq.(4), respectively.

Boundary Conditions

The domain of calculation in the physical plane is semi-infinite (see Fig.1). The flow on the left-hand-side boundary ($x = -\infty$) and on the upper boundary ($y = +\infty$) represents the undisturbed flow. At infinity far downstream of the plate ($x = +\infty$) the flow is assumed to be a parallel flow with non-uniform velocity distribution but constant static pressure $p = 0$. The plate surface and the moving wall are streamlines. Regarding the fact, that the tangential velocity on the wall is equal to $u = 1$, whereas the tangential velocity on the plate surface (PL) is equal to $W_t = 0$, the boundary conditions are:

Plate surface, $-0.5 \le x \le 0.5$, $y = y_{PL}$:

(n = normal on plate surface, subscript t denotes tangential direction)

$$\omega = -\frac{\partial W_t}{\partial n} , \quad \psi = 0, \quad \frac{\partial p_T}{\partial n} = \frac{1}{Re} \frac{\partial^2 W_n}{\partial n^2} \qquad (8)$$

Left-hand-side boundary, $x = -\infty$, $y_w \le y \le +\infty$;
(subscript w denotes values on the wall)

$$\omega = 0, \quad \psi = y + \psi_W, \quad p_T = 0 . \qquad (9)$$

Lower boundary, $-\infty < x < +\infty$, $y = y_w$:

$$\omega = -\frac{\partial u}{\partial y}, \quad \psi = \psi_w, \quad \frac{\partial p_T}{\partial y} = -\omega + \frac{1}{Re} \frac{\partial^2 v}{\partial y^2} \qquad (10)$$

Right-hand-side boundary, $x = +\infty$, $y_w \le y \le +\infty$:

$$\frac{\partial \omega}{\partial x} = 0, \quad \frac{\partial \psi}{\partial x} = 0, \quad p_T = \frac{1}{2}(u^2 - 1) \qquad (11)$$

Upper boundary, $-\infty < x < +\infty$; $y = +\infty$:

$$\omega = 0, \quad \psi = +\infty, \quad p_T = 0 \qquad (12)$$

The Neumann boundary conditions for the total pressure, occuring in eqs.(8) and (10), are derived from the Navier-Stokes equations for stationary flows, regarding the above mentioned boundary conditions for the velocities.

At a first glance the value of the streamfunction at the moving wall, ψ_w, determining the mass flow passing through the

slot between the lower surface of the plate and the moving wall, seems to be an additional unknown. However, as can be shown by application of Green's theoreme, the value ψ_w is determined by the condition, that the circulation around the plate surface has to be equal to zero, or in other words: the non-slip-condition on the complete plate surface can only be satisfied by one value of ψ_w *). The computation of that value ψ_w has to be done iteratively.

Coordinate Transformation

Before numerically evaluating eqs.(1), (2) and (7) the semi-infinite physical domain of Fig.2 is mapped into a finite rectangular domain of computation (see Fig.2) by the transformation

$$x(\xi) = c_1 \frac{\xi}{c_2+(1-c_2)\xi^2-\xi^4}, \quad -\infty < x < +\infty, \quad -1 < \xi < 1, \tag{12}$$

$$y(\eta) = c_3 \frac{\eta}{1-\eta}, \quad y_w < y < +\infty, \quad -0.5 < \eta < 1. \tag{13}$$

The constants $c_1 = 0.375$, $c_2 = 0.25$, $c_3 = -3 \cdot y_w$

were choosen such that the leading edge at $x = -0.5$, and the trailing edge at $x = 0.5$ in the physical plane, are mapped into the points $\xi = -0.5$ and $\xi = +0.5$ respectively, whereas the moving wall is given by the line $\eta = -0.5$ in the computational plane. Besides this, the transformation eq.(12) was developed with the aim to have a more closely packed distribution of grid points in the regions of the leading and trailing edge than in the remaining region of the physical plane. After transformation of eqs.(1), (2) and (7), defining

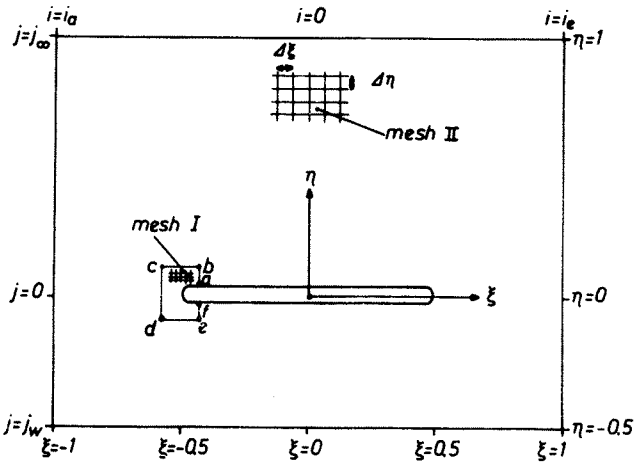

Fig.2 Domain of computation.

$$r = \frac{1}{\frac{\partial x}{\partial \xi}} \tag{14}$$

$$s = \frac{1}{\frac{\partial y}{\partial \eta}} \tag{15}$$

we get

$$\frac{\partial \omega}{\partial t} + r\left(u - \frac{1}{Re}\frac{\partial r}{\partial \xi}\right)\frac{\partial \omega}{\partial \xi} + s\left(v - \frac{1}{Re}\frac{\partial s}{\partial \eta}\right)\frac{\partial \omega}{\partial \eta} = \frac{1}{Re}\left(r^2\frac{\partial^2 \omega}{\partial \xi^2} + s^2\frac{\partial^2 \omega}{\partial \eta^2}\right) \tag{16}$$

$$r^2\frac{\partial^2 \psi}{\partial \xi^2} + s^2\frac{\partial^2 \psi}{\partial \eta^2} + r\frac{\partial r}{\partial \xi}\frac{\partial \psi}{\partial \xi} + s\frac{\partial s}{\partial \eta}\frac{\partial \psi}{\partial \eta} = -\omega(\xi,\eta) \tag{17}$$

$$r^2\frac{\partial^2 p_T}{\partial \xi^2} + s^2\frac{\partial^2 p_T}{\partial \eta^2} + r\frac{\partial r}{\partial \xi}\frac{\partial p_T}{\partial \xi} + s\frac{\partial s}{\partial \eta}\frac{\partial p_T}{\partial \eta} = \omega^2(\xi,\eta) + v \cdot r\frac{\partial \omega}{\partial \xi} - u \cdot s\frac{\partial \omega}{\partial y} \tag{18}$$

The differential boundary conditions in eqs.(8), (10) and (11) are transformed analogously.

Numerical Method

For the numerical integration of the vorticity transport equation the wellknown "Forward-Time-Centered-Space"-Method[1] was applied. It is of first-order accuracy in time and of second-order accuracy in space. The transformed Poisson equations (17) and (18) were discretised using a five-point-formula of second-order accuracy, which converts eqs.(17) and (18) into a set of linear equations. They are solved by the Gauß-Seidel[2] iteration procedure. Of

*) Paper in preparation.

course, there exist more powerful methods for the numerical treatment of eqs.(16) - (18). However, since not much parameters are involved (Reynolds number Re and slot-height h), the above mentioned methods were prefered because of their simplicity with regard to quick programming. The differential boundary conditions in (8), (10) and (11) were discretised using a forward three-point formula.

The fact that the boundary value of the streamfunction on the upper boundary $\eta = 1$ is equal to infinite, requires a special treatment of eq.(17) for the calculation of the streamfunction along the grid line $j = j_\infty - 1$ (see Fig.2). Defining a "transformed" streamfunction ϑ by

$$\vartheta = s \cdot \psi \tag{19}$$

with

$$s = \frac{(1-\eta)^2}{c_3} \tag{20}$$

and $\vartheta \to 0$ for $\eta \to 1$, one gets after introducing eq.(19) into eq.(17) the relation

$$r^2 \frac{\partial^2 \vartheta}{\partial \xi^2} + r \frac{\partial r}{\partial \xi} \frac{\partial \vartheta}{\partial \xi} + s^2 \frac{\partial^2 \vartheta}{\partial \eta^2} - s \frac{\partial s}{\partial \eta} \frac{\partial \vartheta}{\partial \eta} + \left[\left(\frac{\partial s}{\partial \eta} \right)^2 - s \frac{\partial^2 s}{\partial \eta^2} \right] \vartheta = -s \, \omega(\xi, \eta) \tag{21}$$

The discretisation of eq.(21) by second-order difference-formulas, regarding eq.(20) and

$$\frac{\partial s}{\partial \eta} = -2 \frac{1-\eta}{c_3} \tag{22}$$

$$\frac{\partial^2 s}{\partial \eta^2} = \frac{2}{c_3} \tag{23}$$

yields for the grid points $i_a + 1 \le i \le i_e - 1$, $j = j_\infty - 1$, for which

$$1 - \eta = \Delta\eta \tag{24}$$

is valid, the three-point formula

$$r_i \left(r_i \frac{\vartheta_{i+1,j_\infty-1} - 2\vartheta_{i,j_\infty-1} + \vartheta_{i-1,j_\infty-1}}{\Delta\xi^2} + \frac{\partial r}{\partial \xi} \frac{\vartheta_{i+1,j_\infty-1} - \vartheta_{i-1,j_\infty-1}}{2 \cdot \Delta\xi} \right) = - s_{j_\infty-1} \cdot \omega_{i,j_\infty-1} \tag{25}$$

$$i_a + 1 \le i \le i_e - 1,$$

from which the transformed streamfunction ϑ and, by application of eq.(19), the ψ-values may be computed. A similar technique is applied for the calculation of the velocity components $u_{i,j}$ for $i_a + 1 \le i \le i_e$, $j = j_\infty - 1$.

Practical Computation

The domain of computation is subdivided into two regions. Region I, enclosing the leading edge within the lines a - b - c - d - e - f - a has a finer mesh, the mesh in the remaining region II is a coarser one. Both meshes are rectilinear - orthogonal and have constant spacing in the ξ-direction, and in the η-direction, respectively. Due to the smaller mesh sizes the maximal allowable time step in mesh II is smaller, thus requiring multiple performing of computation in mesh I for reaching the time level of mesh II. The flow variables ω and ψ within regions I and II are calculated separately as long as the time level is different in both meshes, using the distribution of ω and ψ along the lines a - b - c - d - e - f - a of the preceding time step as boundary conditions. After the nondimensional time in both regions is the same the distributions of the calculated flow variables ω and ψ are matched along the lines a - b - c - d - e - f - a by the condition that the values of ω and ψ along and their derivates normal to that lines have to be equal for both regions.

Results

Due to the relatively small core storage and the low speed of the computer available the Reynolds number Re had to be restricted to small values. Hence, these results are representative for low speeds only. In Fig.3 the distribution of the shear stress (exerted from the fluid on the wall) and the pressure along the moving wall is given for a Reynolds number Re = 1000 and three different slot heights h/ℓ = 0.04286, = 0.02571, = 0.00857. The plate thicknesses were d/ℓ = 0.03361, = 0.02679, = 0.02598 for these cases.

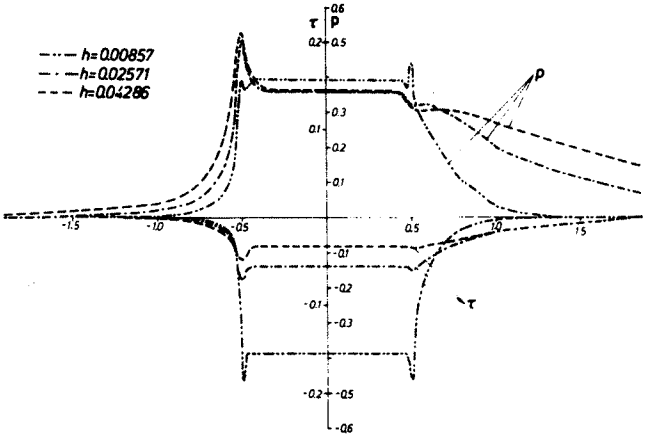

Fig.3 Pressure (p) and shear stress (τ) distributions on the ground for three different slot-heights h/ℓ, Re = 1000.

The magnitude of both the pressure and the shear stress are increasing for the flow approaching the leading edge at x = -0.5. Between $-0.46 \leq x \leq 0.46$ pressure and shear stress are practically constant. They are decreasing downstream of the leading edge (x = 0.5) to the values of the undisturbed flow for $x \to +\infty$. The pressure rise in front of the plate is caused by the displacement effect of the plate and by the fact that the mass flow in the slot between the lower surface of the plate and the moving wall is reduced to approximately half of the mass flow passing through the slot-height-spacing h far upstream of the plate (s. Fig.5). From this a displacement effect is exerted on the whole flow field resulting in a flow circulating around the leading edge from the lower to the upper surface, thus producing the pressure rise at the same time. From Fig.3 can be seen that the shear stress increases with decreasing slot-height h.

The different behaviour of shear stress and pressure distribution for the slot height h = 0.00857 compared with that of the other two other cases, also occuring in the distributions on the plate surface given in Fig.4, is caused by the fact that the mass flow in the slot is reduced to nearly zero due to the very small slot height. Hence, both the plate and the slot may be regarded as one rigid body, building a step of length ℓ on the moving wall.

The pressure distributions along the plate surface, given in the left-hand-side of Fig.4, are showing that a lifting force is exerted from the flow on the flat plate.

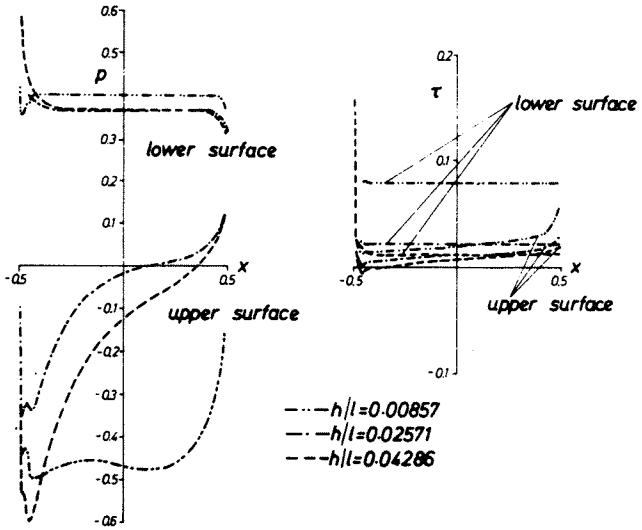

Fig.4 Pressure (p) and shear stress (τ) distributions on the upper and lower surface of the plate for three different slot-heights h/ℓ, Re = 1000.

The magnitude of the shear stress (right hand side of Fig.4) on the lower plate surface is approximately equal to that of the moving wall. The shear stress on the upper surface is, except for the leading edge region, smaller than on the lower surface.

The strong gradients in the pressure and shear-stress distribution of the leading edge region are increasing with decreasing plate thickness. In the case of an infinite thin plate both distributions would deteriorate to a singularity at the sharp leading edge.

In Fig.5 the u-velocity profiles are given for some characteristic stations on the x-axis. The flow is strongly affected by the plate only at a distance less than 50 % of the plate length upstream of the leading edge. Within the slot the velocity distribution is practically linear. The

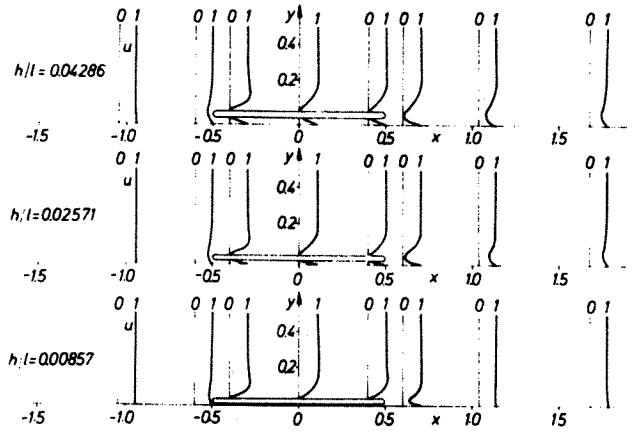

Fig.5 u-velocity profiles for three different slot-heights h/ℓ, Re = 1000.

flow hereinis parallel and similar to a Couette-Flow with a very small negative pressure gradient in the flow direction. The velocity profiles on the uper surface of the plate indicate a flow like boundary layer flow. However, the "boundary-layer-thickness", is of the order of one. Downstream of the trailing edge we have the typical velocity distribution of the near wake.

Conclusion

The incompressible laminar flow past a flat plate moving at a small distance parallel to the ground was investigated theoretically. The flow field is calculated by numerical integration of the vorticity transport equation and the Poisson equation for the streamfunction. The computed results show that for a Reynolds number of about 1000 (related to the plate length) the flow in the slot between the lower surface of the plate and the moving wall is a Couette flow with a small negative pressure gradient in the flow direction for a range of slot heights between 0.8 % and 5 % of the plate length. Within the slot a pressure rise is induced by the viscous effects of the flow, from which a lifting force is exerted on the plate. The present investigation is a fore runner for the investigation of the flow in a threedimensional slot of finite length and finite width. The computation-method for that case is in development but no results are available up to now.

References

[1] Roache, P.J., "Computational Fluid Dynamics," Hermosa Publishers Albuquerque, 1972.

[2] Zurmuehl, R., "Praktische Mathematik," Berlin-Heidelberg-New York: Springer, 1965.